Light Metals 2015
Edited by: Margaret Hyland
TMS (The Minerals, Metals & Materials Society), 2015

THE INFLUENCE OF COOLING RATE AND ALLOYING ELEMENTS ON THE MICROSTRUCTURE REFINEMENT OF Al-5Fe ALLOY

Y. L. Liu, M. Liu, L. Luo, L. Zhang, Y. H. Zhao, J. J. Wang, C. Z. Liu[1]

Shenyang Aerospace University, 37 Daoyi Avenue S., Shenyang, China

Keywords: aluminum alloys, Al-Fe alloy, rapid solidification, microstructure, intermetallics

Abstract

This research was focused on refining the microstructures of Al-5Fe alloy by increasing cooling rate during solidification and adding alloying elements. Under the condition of near-rapidly solidification, the primary $Al_{13}Fe_4$ phase was refined to the order of magnitude of 10 microns. Adding silicon to the alloy resulted in changes to the morphologies of the primary phase from star-like pattern to polygonal and firework-like patterns. The addition of silicon and cerium gave rise to further refinement in both primary and eutectic iron-rich phases to a significant extent.

Introduction

Aluminum-iron alloy is an excellent candidate for industrial use at elevated temperature. However, hypereutectic Al-Fe sheet material normally cannot be produced by the ingot-rolling procedure due to the poor formability caused by the coarse $Al_{13}Fe_4$ intermetallics, which form during ingot casting. Since the solubility of iron in aluminum is very low (<0.052wt pct)[1], this causes the formation of the compound $Al_{13}Fe_4$ as both the primary and eutectic phase in hypereutectic Al-Fe alloy. The mechanical properties and formability of the alloy are strongly dependent upon the size, morphology, and distribution of this compound. Coarse structures of $Al_{13}Fe_4$ lead to the reduction of the mechanical properties and formability of the alloy. On the other hand, $Al_{13}Fe_4$ is stable at elevated temperature. Therefore, finely dispersed $Al_{13}Fe_4$ can greatly improve alloy properties, especially, at elevated temperature.

The microstructure of the $Al_{13}Fe_4$ compound is a function of the cooling rate and chemical composition of the alloy. The solidification of the Al rich Al-Fe system has been studied under the conditions of rapid quenching [2-6], mechanical alloying[6-8] and severe plastic deformation (SPD)[9-12]. The results indicated that rapid solidification was an effective method in refining the intermetallic compounds. Adding alloying elements was another effective way of refining the intermetallic compounds. Zhou et al [13] and Liu et al [14] considered that the morphology of primary Al_3Fe phase in Al-5Fe alloy could be improved appreciably by adding alloying element. Cerium is a rare earth element which was often added in the rapid solidification of Al-Fe alloys [15-17] and showed positive effects on the alloy properties.

Although rapid solidification is effective in refining casting structures, the process of rapid solidification is complicated and has been limited to small samples. Compared to rapid solidification, near-rapid cooling, which refers to a cooling rate between $10^0 - 10^3$ °C s^{-1}[18], is easy to achieve and can be applied to commercial quantities. For example, continuous strip casting is a near-rapid solidification process. If, through near-rapid solidification, the Al-5Fe alloy can be refined to the extent that the cast material can be subject to further cold work, then sheet material of this alloy can be produced using the continuous strip casting process. This will be of great progress in the development of Al-Fe alloy. However, there is minimal literature on the structure and morphology of iron-containing phases formed under near-rapid cooling. It is worth investigating the refinement of the intermetallic compounds of hypereutectic Al-Fe alloy using near-rapid solidification (cooling) technology. This research focused on the effect of the cooling rate and alloying elements Si and Ce on the microstructure of Al-5Fe alloys. The aim was to refine the intermetallic compounds of Al-5Fe alloy to such an extent so that the alloy could be subject to further cold work.

Experimental Procedures

The Al-5wt%Fe alloy (Alloy 1) used in this study was prepared by melting 500g of commercial pure aluminum (99.7 wt%) and 500g of Al-10wt%Fe master alloy in a clay graphite crucible in a 5kW well-type resistance furnace. The melt was held for 30 minutes at 900°C and stirred every 10 minutes. After degassing and dross skimming, the melt was poured into different molds to obtain different cooling rates. Cooling curves were created by recording temperature evolution every 0.1 second. The average cooling rates before the start of solidification were calculated by using the formula dT/dt and were computed from the approximate straight line portion of the cooling curve. The following four cooling conditions were created.

- Sample 1: cooled in furnace in alumina crucible, cooling rate: 0.037°C s^{-1}
- Sample 2: cooled in air in alumina crucible, cooling rate: 1.88°C s^{-1}
- Sample 3: cast in an iron mold, casting size: 60X40X9.5 mm, cooling rate: 35.2°C s^{-1}
- Sample 4: cast in a double-side water cooled iron mold, casting size: 60X40X9.5 mm, cooling rate: 157.8°C s^{-1}.

The Al-5wt%Fe-3wt%Si alloy (Alloy 2) was prepared by melting commercial pure aluminum (99.7wt%Al), Al-10wt%Fe and Al-30wt%Si master alloys. The Al-5wt%Fe-3wt%Si-1.0wt%Ce alloy (Alloy 3) was prepared by melting commercial pure aluminum (99.7wt%Al), Al-10wt%Fe, Al-30wt%Si and Al-10wt%Ce master alloys. The melts of alloy 2 and alloy 3 were cast in the iron mold, as the same as Sample 3 of alloy 1, as mentioned above, casting size: 60X40X9.5 mm, cooling rate: 35.2°C s^{-1}. The chemical compositions of the prepared alloys were then analyzed.

Metallographic samples were cut from the cast samples in the vicinity of the thermocouple's tip, prepared with standard metallographic procedures and etched with 0.5 vol.% HF + 99.5 vol.% H_2O solution. The microstructures of the samples were examined using an Olympus GX71 optical microscope. A Zeiss scanning electron microscopy with Oxford energy dispersive X-

ray (EDX) analyzer was employed to identify intermetallic compounds.

Result and Discussion

The first part of the research was to investigate the influence of cooling rates on the as-cast microstructures of Al-5Fe alloy. Under the condition of slow cooling in Sample 1 (0.037°C s^{-1}), the primary iron-rich phase and the eutectic iron-rich phase displayed bulk blocky and long strip-like morphologies, respectively, see Figure 1(a). The long strips were composed of many clusters with each cluster representing a grain. In Sample 2, solidified at a cooling rate of 1.88°C s^{-1}, the primary iron-rich phase changed to willow leaf-like; the eutectic iron-rich phase still kept the long strip characteristics, see Figure1(b), but their sizes were much smaller (approximately one-fifth) compared to Sample 1. The EDX analyses indicated that both the primary and the eutectic iron-rich phases in both Sample 1 and Sample 2 were intermetallic $Al_{13}Fe_4$, see Table 1.

When the cooling rate was increased to 35.2°C s^{-1} (Sample 3) which was within the range of near-rapid cooling, the primary phase showed irregular star-like morphology; the eutectic phase changed to short rod or particle-like structures, which formed chains along grain boundaries, or clusters within triangle grain boundaries and inter-dendrite, as shown in Figure 1(c). Both primary and eutectic phases were further significantly refined by near-rapid cooling. Figure 1(d) shows the as-cast microstructures of Sample 4, solidified at a cooling rate of 157°C s^{-1}. Both primary and eutectic intermetallics were refined to an even greater extent than Sample 3.

Under the condition of near-rapid solidification (Sample 3 and Sample 4), although some star-like structures of the primary intermetallics had relatively large size, most primary intermetallics appeared as small star-like blocks. The sizes of these small star-like blocks were less than the order of magnitude of 10 microns. Table 1 also provided the results of the EDX analyses on the iron-rich phases in Samples 3 and 4. The primary phase still kept the $Al_{13}Fe_4$ constitutive formula, however the composition of the eutectic iron-rich phase was lowered to approximately Al_6Fe. Under the condition of near-rapid cooling, the eutectic intermetallic changed from $Al_{13}Fe_4$ to Al_6Fe. This result agreed with the general opinion that a faster cooling rate favored the formation of metastable Al_6Fe phase.

Increasing cooling rate from 0.037°C s^{-1} to 1.88°C s^{-1} did not change the property of the microstructure of the alloy; but the size of the eutectic $Al_{13}Fe_4$ reduced greatly. Increasing cooling rate to near-rapid cooling resulted in a significant refinement in the as-

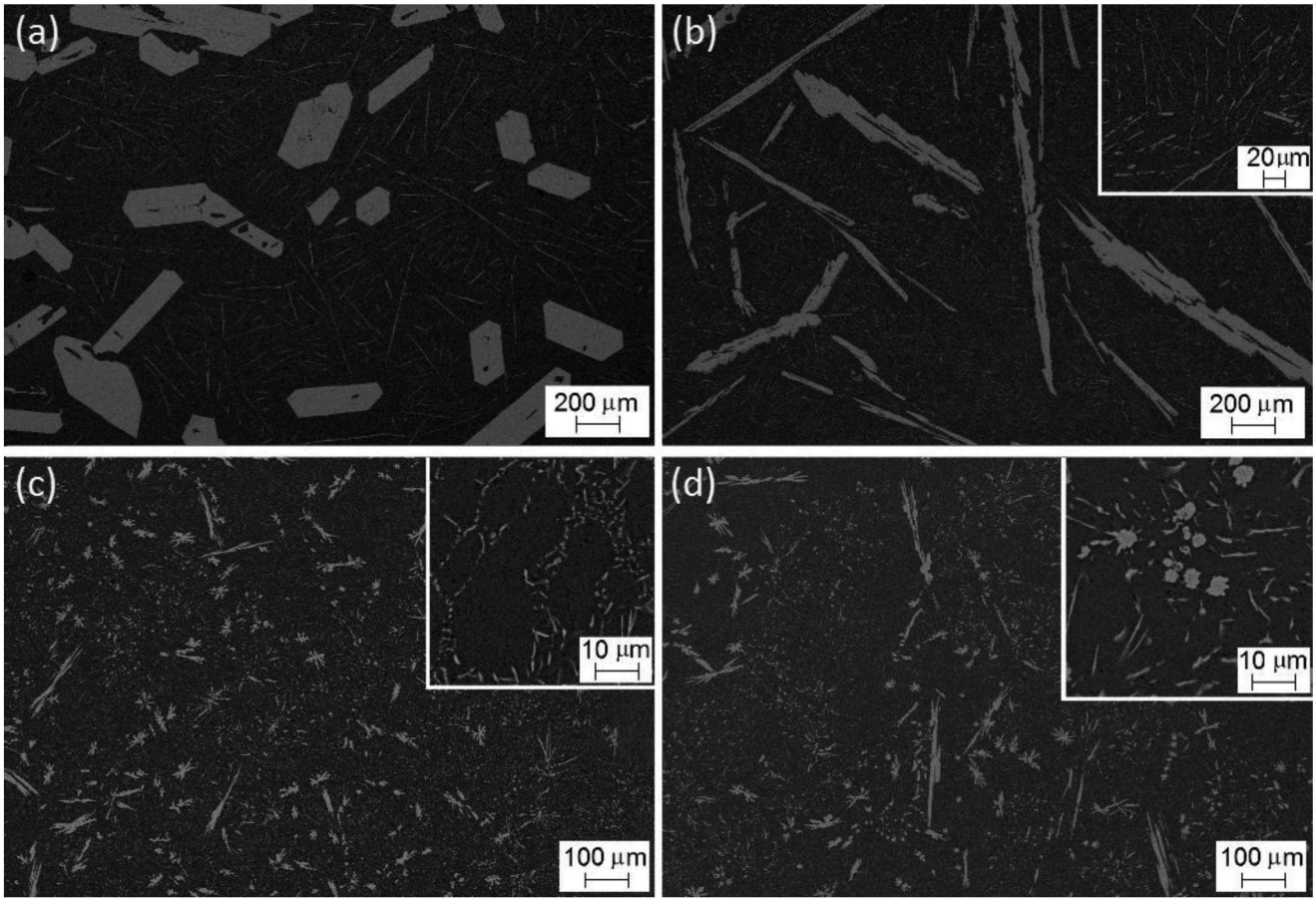

Figure 1 The microstructures of the Al-5Fe alloy solidified at
(a) 0.037°C s^{-1}; (b) 1.88°C s^{-1}; (c) 35.2 °C s^{-1}; (d) 157.8 °C s^{-1}.
(b) The inset images are the high magnification images of the eutectic iron-rich phases

Table 1 Compositions of iron-rich phases analyzed by EDX, at%

Sample	Intermetallic	Al	Fe	Phase
Sample 1	Primary	75.08	24.92	$Al_{13}Fe_4$
	Eutectic	75.98	24.02	$Al_{13}Fe_4$
Sample 2	Primary	77.63	22.37	$Al_{13}Fe_4$
	Eutectic	80.63	19.37	$Al_{13}Fe_4$
Sample 3	Primary	77.12	22.88	$Al_{13}Fe_4$
	Eutectic	85.90	14.10	Al_6Fe
Sample 4	Primary	76.69	23.31	$Al_{13}Fe_4$
	Eutectic	87.45	12.55	Al_6Fe

cast microstructures of the alloy. This result would encourage the attempt of producing wrought Al-Fe alloy for industrial use. The cooling rate of 35°C s^{-1} is in the range of the cooling rate for continuous strip casting process. Therefore, it is expected that the fine primary and eutectic iron-rich phase could be achieved by continuous strip casting process.

Adding alloying elements to the Al-5Fe alloy was the second attempt of refining the as-cast microstructure. Figure 2 shows the as-cast microstructure of Alloy 2 (with 3w% silicon addition) solidified at a cooling rate of 35°C s^{-1}. The addition of 3wt% silicon significantly altered the microstructure of the Alloy. For the primary phase, the irregular star-like structures were similar to the primary $Al_{13}Fe_4$ in Sample 3 in both size and morphology. The other two polygonal and firework like patterns should also be the primary phase. The EDX analysis indicated that these two phases were also $Al_{13}Fe_4$ phase, with minimal silicon, see Figure 2(d and e) for the EDX spectrums. The silicon content was 2.47at% in the firework like pattern phase and 6.09at% in the polygonal phase.

Figure 2(b and c) shows the fine compounds. There existed two kinds of fine compounds distinguished by color (light gray and black). The EDX analysis indicated that the fine compound in light gray contained Al, Fe and Si. The content of silicon was 5.0 – 6.0at%, iron was 9.0 – 11.0at%. The ratio between silicon and iron was approximately 1:2. Therefore, it was assumed that this compound was Al_8Fe_2Si. The compound in black contained mainly silicon, which should be the silicon phase.

The morphology change of the primary phase was attributed to the addition of silicon to the alloy. According to Al-Fe-Si phase diagram [19], as shown in Figure 3, for the Al-5Fe-3Si alloy, the primary phase was $Al_{13}Fe_4$. During solidification, the primary $Al_{13}Fe_4$ phase first precipitated, which caused the silicon atoms to move to the interface front. Under the condition of near-rapid cooling, the silicon atoms would build up a layer at the interface front since they would not have enough time to diffuse away. As a result, the diffusion of iron atoms toward the growing primary $Al_{13}Fe_4$ would be blocked by the barrier of the silicon layer and, hence, the growth of the primary $Al_{13}Fe_4$ was retarded and its morphology changed from irregular star-like to small blocky. The small blocky phases constituted a cluster of firework like patterns. On the other hand, the fast growing primary $Al_{13}Fe_4$ might trap some silicon. Should a high percentage of silicon be trapped in the $Al_{13}Fe_4$ phase, for example in the polygonal phase, the buildup of silicon atoms in the interface front would decrease. As a result, the resistance for iron atoms to diffuse to the growing $Al_{13}Fe_4$ phase would be reduced; and the size of the primary $Al_{13}Fe_4$ phase could continue to grow. Therefore, the primary $Al_{13}Fe_4$ grew in polygonal shape to a relatively large size.

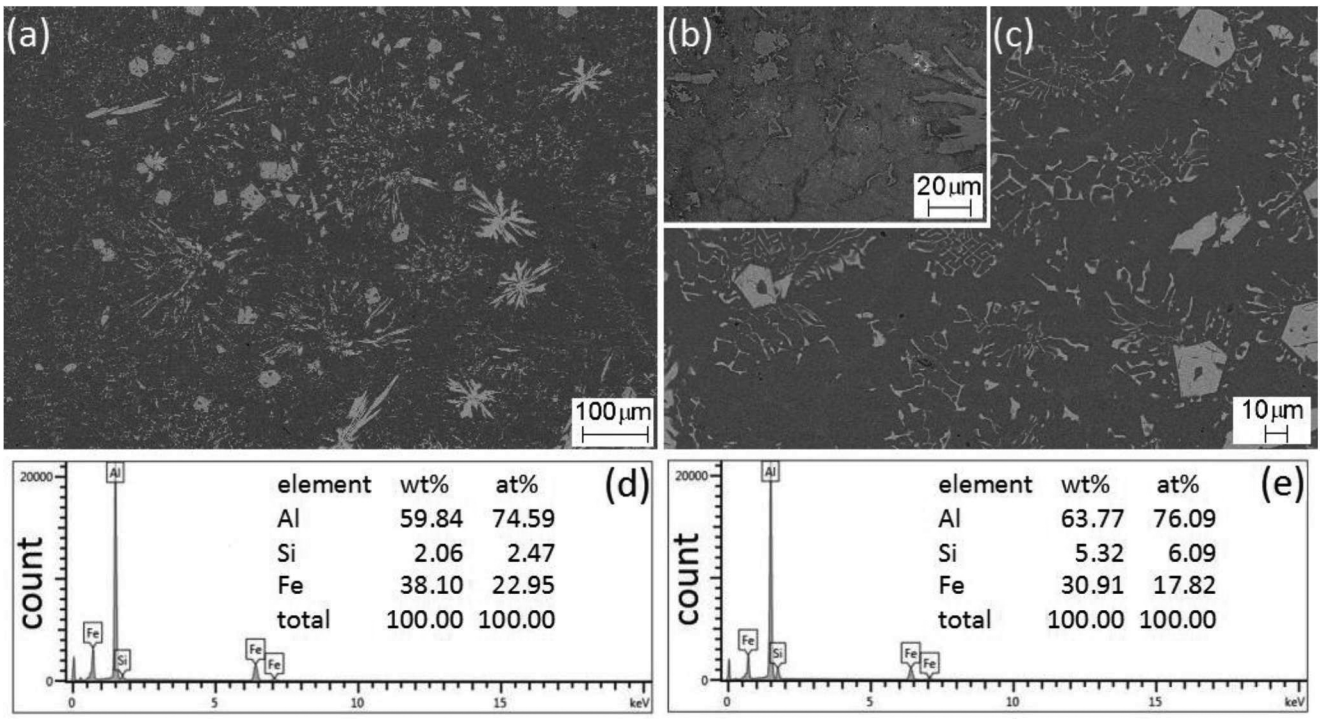

Figure 2 The microstructures of the Al-5Fe-3Si alloy solidified at 35°C s^{-1}
(a) Primary phase; (b) eutectic silicon; (c) Al_8Fe_2Si phase; (d) EDX spectrum of the small blocky primary phase; (e) EDX spectrum of the polygonal primary phase

The solidification path of the Al-5Fe-3Si alloy is quite complex. According to the Al-Fe-Si phase diagram[19], see Figure 3, it starts with the precipitation of primary $Al_{13}Fe_4$, then ternary peritectic reactions L + $Al_{13}Fe_4$ → α-Al + α-Al_8Fe_2Si (τ_5) follows, then ternary peritectic reactions L + α-Al_8Fe_2Si → α-Al + β-Al_5FeSi (τ_6) follows, finally, ends with ternary eutectic reaction L → α-Al + β-Al_5FeSi (τ_6) + Si. But from the backscatted image of the microstructure of Alloy 2 (Figure 2), the β-Al_5FeSi phase did not appear. In addition, from the inset image of Figure 2(b), the eutectic silicon was divorced to the grin boundaries, no third eutectic compound was observed around the eutectic silicon. It is assumed that eutectic silicon formed from binary eutectic reaction, instead of ternary eutectic. It is assumed that under the condition of near-rapid solidification, the formation of intermetallic β-Al_5FeSi was suppressed.

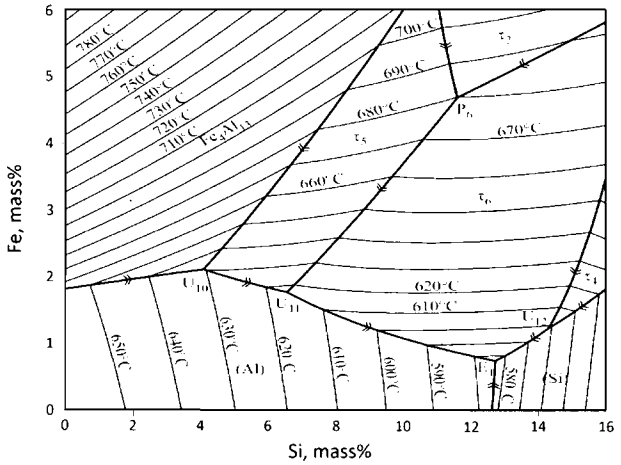

Figure 3 The phase diagram of Al-Fe-Si system at Al corner[19]

Alloy 3 was based on Alloy 2 with an addition of 1.0wt% Ce. After solidification at a cooling rate of 35°C s^{-1}, the as-cast microstructures were quite complicated. The primary phase changed in morphology, size and distribution, as shown in Figure 4. The majority of the phase was in leaflike or flake shapes; small amount of polygonal blocks were also observed; but the star-like morphology which appeared in Alloy 2 was difficult to find. Comparing Figure 4(a) to Figure 2(a), it could be seen that the sizes of the leaflike or flakes phase in Alloy 3 were much smaller, which indicated that the addition of Ce led to the reduction of the size of the primary phase.

Figure 4(b) and (c) showed the eutectic compounds in Alloy 3. Other than the fine α-Al_8Fe_2Si with Chinese script type morphology, which was similar to the ones observed in Alloy 2, there were two more fine structures: both in rod shape. The white rod contained Al, Si and Ce; the gray rod contained Al, Fe and Si. Results of the EDX analysis are listed in Table 2. The composition of the Al-Si-Ce phase agreed with none of the known ternary phases in the Al-Si-Ce system [20, 21]. Further work is needed to determine the structure of this phase. The composition of the gray rod was close to the phase β-Al_5FeSi.

Rare earth cerium is of great influence on the solidification microstructure of the Al-Fe-Si alloy. In Alloy 3, the primary $Al_{13}Fe_4$ phase was further refined to a great certain extent compared to Alloy 2. Therefore, it is confirmed that cerium is an

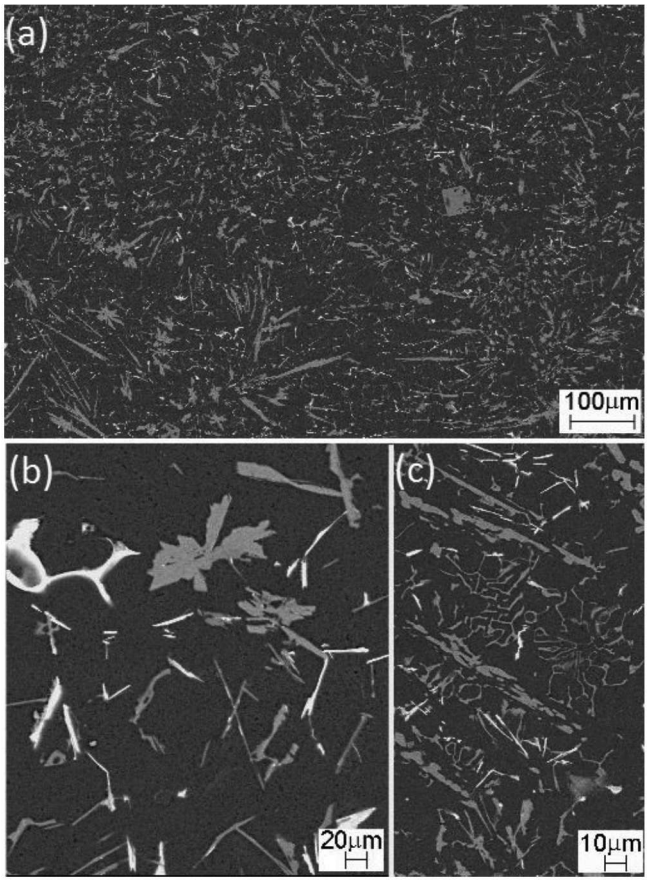

Figure 4 The microstructures of the Al-5Fe-3Si-0.5Ce alloy solidified at 35°C s^{-1}
(a) Primary phase; (b) the rod-like AlSiCe phase (white) and β-Al_5FeSi phase (gray); (c) Al_8Fe_2Si phase

Table 2 Compositions of iron-rich phases analyzed by EDX, at%

Phase	Al	Fe	Si	Ce
Primary phase	73.79	21.84	2.38	
Gray rod	78.48	9.21	12.1	
Which rod	42.59		33.12	24.29

effective alloying element in refining microstructure of Al-Fe alloys. Further work will be carried out to investigate the formability and mechanical properties of the alloy with cerium addition.

Conclusions

In summary, the as-cast microstructures of the Al-5Fe alloy were refined to a significant extent by using near-rapid solidification technology. The primary $Al_{13}Fe_4$ in small star-like blocks were in the order of magnitude of 10 microns in size.

Adding silicon resulted in the change of the morphologies of primary phase from star-like to polygonal and firework-like pattern; the addition of silicon and cerium gave rise to the refinement in both primary and eutectic iron-rich phases to a great extent.

Acknowledgement

The authors are grateful to the Research Foundation of Shenyang Aerospace University for its financial support.

References

1. U.R. Kattner, B.P. Burton, ASM Handbook, Vol. 3: Alloy Phase Diagrams, ASM, Materials Park, OH, 1992, pp. 2-44.
2. S.D. Kaloshkin, V.V. Tcherdyntsev, et al, Mater. Trans. JIM, 43(2002), pp. 2031-2038.
3. Y.H. Zhang, Y.C. Liu, et al, J. Alloys Compd., 473(2009)442-445.
4. V.V. Tcherdyntsev, S.D. Kaloshkin, et al, Mater. Sci. Eng. A, 375-7(2004) pp. 888-893.
5. D.K. Mukhopadhyay, C. Suryanarayana, F.H. Froes, Metall. Mater. Trans. 26A(1995) pp. 1939-1946.
6. S. S. Nayak, B. S. Murty, S. K. Pabi, Bull. Mater. Sci, 31(2008)3, pp.449-454
7. Dmitri V. Malakhov, Damon Panahi, Mark Gallerneault, CALPHAD, 34 (2010) pp.159-166
8. S.S. Nayak, M. Wollgarten, et al, Mater. Sci. Eng. A, 527(2010)9 pp, 2370-2378
9. O. N. Senkov, F.H. Froes, V.V. Stolyarov, et al,? Scripta Mater, vol. 38(1998), pp. 1511-1516.
10. O.N. Senkov, F.H. Froes, V.V. Stolyarov, et al, Nanostruct. Mater, 10(1998), pp. 691-698.
11. V.V. Stolyarov, R. Lapovok, et al, Mater. Sci. Eng. A, 357(2003), pp. 159-167.
12. Jorge M. Cubero-Sesin, Zenji Horita, Metal. Mater. Trans 43A(2012) pp.5182-5192
13 Z. P. Zhou and R. D. Li, Acta Metallurgica Sinica, 39(2003) pp.608-612
14 Bo Liu, Xiao-Guang Yuan, Hong-Jun Huang, JOM, 64(2012)2, pp. 316-322
15. U. Prakash, T. Raghu, et al, J. of Mater. Sci., 34(1999)20, pp 5061-5065
16. M. Fass, D. Eliezer, et al, , J. of Mater. Sci., 33(1998)3, pp 833-837
17. O. D. Neikov, Yu. V. Mil'man, et al, Powder Metallurgy and Metal Ceramics, 46(2007)9-10, pp 429-435
18. M.C. Flemings, in: J. E. Lait, I. V. Samarasekera (eds), Proceedings of the F. Weinberg International Symposium on Solidification Processing, (1990), pp. 173-194
19. Gautam Ghosh, in: Effenberg G, Ilyenko S (Eds.), Light Metal Systems, Part 2, Londolt-Bornstein New Series IV/11A2, Springer, Berlin Heidelberg, (2005), pp. 359-409
20. H. Flandorfer, D. Kaczorowski, et al, J. of Solid State Chemistry, 137(1998)2, pp. 191-205
21. V. Raghavan, J. of Phase Equilibria and Diffusion, 28(2007)5, pp 456-458